

density-of-states curve which should be more Gaussian in character than in bcc iron. In a calculation, in I, for fcc iron with a Gaussian density of states, it was found that the shielding of the 3s electron by *d*-like electrons could lead to smaller values of $\Psi_{3s}^2(0)$ as the volume decreased. Such a behavior would counteract the expected increase in $\Psi_{4s}^2(0)$.

We feel the above treatment permits a reasonable

qualitative understanding of the data. On the other hand, a more realistic treatment of the impurity problem and its relation to the volume should be attempted.

ACKNOWLEDGMENTS

The authors are grateful to P. G. Debrunner, H. Frauenfelder, M. Atac, P. A. Beck, and J. J. Pinajian for their assistance in various phases of this work.

Far-Infrared Optical Absorption of Fe²⁺ in ZnS

GLEN A. SLACK, S. ROBERTS, AND FRANK S. HAM

General Electric Research and Development Center, Schenectady, New York

(Received 21 October 1966)

The optical absorption of substitutional Fe²⁺ impurities in natural single crystals of cubic ZnS has been measured in the far infrared (10 to 100 cm⁻¹) at temperatures from 4 to 25°K. Several absorption peaks are identified with electric- and magnetic-dipole transitions between the five spin-orbit levels of the ⁵E ground term of tetrahedral Fe²⁺. The positions and absolute intensities of these peaks agree reasonably well with crystal field theory and with values obtained for the various parameters from previous measurements of the optical absorption in the near infrared. The separation *K* of the spin-orbit levels of the ⁵E term is found to be 15.2±0.4 cm⁻¹. Oscillator strengths for the transitions are in the range 5×10⁻⁹ to 5×10⁻⁸. Lifetimes for spontaneous radiative decay of the excited levels are calculated to be of the order of ½ to 30 h, and actual lifetimes are therefore determined by nonradiative processes. These observations support the conclusion that no pronounced Jahn-Teller effect occurs in the ⁵E state of Fe²⁺ in ZnS.

I. INTRODUCTION

THE present work is a study of the optical absorption of Fe²⁺ impurities in ZnS crystals at low temperatures in the far infrared. The measurements were made on natural crystals of cubic ZnS at temperatures between 4 and 25°K in the wavelength range from 100 to 1000 μ (wave number 10 to 100 cm⁻¹). Previous studies^{1,2} of the low-temperature thermal conductivity of crystals of CdTe and MgAl₂O₄ containing Fe²⁺, and studies³ of the optical absorption in the near infrared of Fe²⁺ impurities in ZnS, CdTe, and MgAl₂O₄ have shown that there exist low-energy excited states of the Fe²⁺ ions lying in the range 10 to 100 cm⁻¹ above the ground state. If light may induce transitions to these excited levels from the ground state, or among these excited levels when they are thermally populated, then absorption peaks should be observed in this region of the far infrared. In the work reported here, several such absorption peaks are found for Fe²⁺ in cubic ZnS, and their positions and intensities are compared with theory.

The Fe²⁺ impurity ions substitute for Zn²⁺ ions in natural crystals³ of cubic ZnS and thus occupy lattice sites of tetrahedral symmetry. The ground term of Fe²⁺ (3d⁶) should then be ⁵E, which is split in second

order by spin-orbit interaction. The previous optical studies³ of the fine structure of the ⁵E → ⁵T₂ absorption band supported the predictions of crystal field theory for the ⁵E term,⁴ indicating that ⁵E is split into five uniformly spaced spin-orbit levels with an interval of about 15 cm⁻¹. These results indicated that Fe²⁺ in ZnS does not undergo a static Jahn-Teller distortion in the ⁵E state. While a dynamical Jahn-Teller effect was proposed³ to account for the levels found for the ⁵T₂ state and may be present as well in ⁵E, no evidence was obtained that indicated that such an effect was strong enough in ⁵E to cause any marked change in the spin-orbit splitting of this state from that given by crystal field theory. These conclusions are given further support by the results of the present investigation.

Earlier studies⁵⁻¹⁰ of optical reflectivity and absorption within the wavelength range examined in the present work have been reported for ZnS but have been concerned with ZnS itself and not with impurity ab-

⁴ W. Low and M. Weger, *Phys. Rev.* **118**, 1119 (1960).

⁵ T. Liebisch and H. Rubens, *Sitzber. Preuss. Akad. Wiss.* **1919**, 876 (1919); **1921**, 211 (1921).

⁶ J. Strong, *Phys. Rev.* **38**, 1818 (1931).

⁷ W. M. Sinton and W. C. Davis, *J. Opt. Soc. Am.* **44**, 503 (1954).

⁸ H. Yoshinaga and R. A. Oetjen, *J. Opt. Soc. Am.* **45**, 1085 (1955).

⁹ H. Yoshinaga, *Phys. Rev.* **100**, 753 (1955).

¹⁰ M. Balkanski, M. Nusimovici, and R. Le Toullec, *J. Phys. (Paris)* **25**, 305 (1964).

¹ G. A. Slack and S. Galginitis, *Phys. Rev.* **133**, A253 (1964).

² G. A. Slack, *Phys. Rev.* **134**, A1268 (1964).

³ G. A. Slack, F. S. Ham, and R. M. Chrenko, *Phys. Rev.* **152**, 376 (1966).

sorption bands. These previous studies were made at 300°K over the range 40 to 500 cm^{-1} . They showed that ZnS is reasonably transparent from 40 to 150 cm^{-1} at 300°K and that the reflection loss at one surface is about 25%. No previous work on the absorption bands of impurities in ZnS or any other II-VI compounds in the 10 to 100 cm^{-1} region is known. There have been reports on the far-infrared absorption spectra of transition and rare-earth metal impurities in other compounds.¹¹⁻¹⁴

In this paper we first describe the experimental techniques and present the experimental results. The theory for the spin-orbit levels of the 5E state is then reviewed, and the theoretical predictions for the oscillator strengths of electric and magnetic-dipole transitions among these levels are developed. These predictions are compared with the experimental values in the final section of the paper.

II. SAMPLES AND EXPERIMENTAL TECHNIQUE

The far-infrared measurements were made using a ruled grating monochromator described previously by Roberts and Coon.¹⁵ Radiation from the monochromator was admitted to a helium cryostat containing the sample and the detector through a 12-mm-diam vertical light pipe. The samples were placed over openings on a horizontal turntable in a chamber held at a fixed temperature in the liquid-helium or liquid-hydrogen range. This turntable was arranged so that any of several samples or a blank hole could be placed in the path of the radiation. A germanium bolometer, mounted in a separate chamber below the sample, was used to detect and measure the transmitted radiation. The bolometer was operated in surroundings at about 1.1°K, independent of the temperature of the sample. In order to stabilize their temperatures, the sample and the bolometer were maintained in helium gas at a nominal pressure of 100 mTorr. Sample temperatures were measured with carbon-resistance and wire-wound copper-resistance thermometers.

The eight different single-crystal samples were cut in the shape of flat disks, with an area of 1.3 cm^2 and thicknesses of 0.2 to 0.4 cm. The surfaces were polished to mirror smoothness under visible light, and the two flat faces were cut with an angular tilt of from 1° to 3° of arc. This tilt helped to reduce interference effects which occur in thin samples at these long wavelengths. Four

TABLE I. Description of the single crystals of natural cubic ZnS .

| Sample no. | Source | Color in bulk | a_0^a | Impurity concentration ^b | | | | |
|------------|-----------------------------------|---------------|---------|-------------------------------------|----|------|------|--------|
| | | | | Fe | Cd | Mn | Co | Others |
| R118 | Picos de Europa, Santander, Spain | Yellow | 5.412 | 41 | 10 | <0.2 | <0.2 | <0.2 |
| R140 | Shiraita, Echigo, Japan | Yellow-brown | 5.411 | 350 | 45 | 9 | 3 | ≤1 |

^a X-ray lattice parameter in Å.

^b The Fe concentration was determined by a solution colorimeter, the others by an emission spectrograph. The concentrations are given in units of 10^{18} atoms/ cm^3 .

samples each were cut from two different large single crystals of cubic ZnS , labeled R118 and R140. These large crystals are described in Table I. Both were single crystals of cubic ZnS containing iron, and were obtained from natural mineral deposits. The optical absorption of these samples in the near infrared and visible from 1000 to 35 000 cm^{-1} at 300°K and below has been reported previously.³ These results showed that most, if not all, of the iron impurities were in the form of Fe^{2+} substitutionally incorporated for Zn^{2+} .

The relative transmissivity of the sample at different wave numbers $\bar{\nu}$ was determined by comparing the response of the bolometer to the radiation passing through the sample to that received when the blank hole in the turntable was substituted for the sample. The absolute transmissivity could not be determined so easily, however, because the temperature and sensitivity of the bolometer varied as the sample was moved, and it was difficult to correct for this change. The transmissivity T of a sample with plane, nearly parallel faces is related to the absorption coefficient α by

$$T = \frac{I_T}{I_0} = \frac{(1-R)^2 e^{-\alpha t}}{1 - R^2 e^{-2\alpha t}}, \quad (1)$$

where I_T denotes the intensity of the transmitted light beam, I_0 the intensity of the incident light beam, R the fraction of energy reflected at normal incidence at one ZnS -air interface, and t the sample thickness. Interference effects were neglected in deriving Eq. (1), and they were not observed in our wedge-shaped samples. The second term in the denominator has a maximum value of about 0.05, and this term was left out in calculating the results of our experiments. In the present case, R may be calculated directly from the index of refraction and is nearly constant in the wave-number range considered. The wave-number dependence of α was therefore determined by the relative transmissivity at different wave numbers. An absolute reference was estimated by assuming that $e^{-\alpha t}$ was very close to unity for $\bar{\nu} < 10 \text{ cm}^{-1}$.

A survey of the data in the literature on the low-

¹¹ A. Hadni, Phys. Rev. **136**, A 758 (1964).

¹² J. C. Hill and R. G. Wheeler, Phys. Rev. **152**, 482 (1966).

¹³ E. D. Nelson, J. Y. Wong, and A. L. Schawlow, Phys. Rev. (to be published).

¹⁴ J. Y. Wong, M. J. Berggren, and A. L. Schawlow, in Proceedings of the Johns Hopkins Conference on Optical Properties of Ions in Crystals, Baltimore, 1966 (to be published).

¹⁵ S. Roberts and D. D. Coon, J. Opt. Soc. Am. **52**, 1023 (1962).

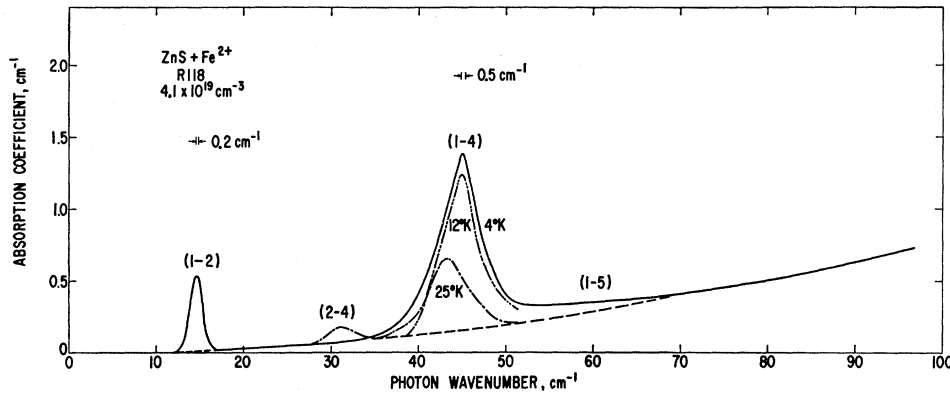


FIG. 1. The optical absorption coefficient of natural cubic ZnS crystal R118 versus wave number at several temperatures. The transitions principally responsible for the various peaks are indicated by (A-B). The spectrometer resolution is indicated.

frequency dielectric constant¹⁶⁻¹⁸ of ZnS and on the far-infrared index of refraction $n^{5,9,10,19-21}$ yields a range of values from 2.74 to 2.95. We choose $n = 2.88 \pm 0.04$ for the wave-number range from 0 to 100 cm^{-1} , and assume that it is independent of temperature. This value is used to estimate the reflection loss at normal incidence. It also enters the calculation of the experimental values for the oscillator strengths of the various Fe^{2+} absorption lines, and from the relation²²

$$(\mathcal{E}_{\text{eff}}/\mathcal{E}) = (n^2 + 2)/3 \quad (2)$$

it determines the value which we have used for the local field correction $(\mathcal{E}_{\text{eff}}/\mathcal{E})$ at the Fe^{2+} site.

III. EXPERIMENTAL RESULTS

The measured absorption coefficient $\alpha(\bar{\nu})$ is shown as a function of photon wave number $\bar{\nu}$ in Figs. 1 and 2, for several temperatures. Several absorption peaks are observed, and these are labeled in the figures by a pair of numbers (A-B) according to the pair of levels of 5E which is presumed to be principally responsible for the peak (see Secs. IV and V). The wave numbers of these peaks, together with their peak heights and half-widths, are given in Table II. Also given in Table II for each peak is the normalized intensity I defined by

$$I = \frac{mc^2 n}{\pi e^2 N} \left(\frac{\mathcal{E}}{\mathcal{E}_{\text{eff}}} \right)^2 \int \alpha(\bar{\nu}) d\bar{\nu}, \quad (3)$$

the integral being taken over the region of the peak after $\alpha(\bar{\nu})$ has been corrected for the background absorption of the ZnS. In Eq. (3), N is the number of

¹⁶ W. Schmidt, *Ann. Physik* **9**, 919 (1902).

¹⁷ J. Takubo, *Mem. Sci. Kyoto Univ.* **B16**, 95 (1941).

¹⁸ D. Berlincourt, H. Jaffee, and L. R. Shiozawa, *Phys. Rev.* **129**, 1009 (1963).

¹⁹ E. Burstein and P. H. Egli, in *Advances in Electronics and Electron Physics*, edited by L. Marton (Academic Press Inc., New York, 1955), Vol. 7, p. 1.

²⁰ F. Abeles and J. P. Mathieu, *Ann. Phys. (Paris)* **3**, 5 (1958).

²¹ T. Deutsch, in *Proceedings of the International Conference on Semiconductor Physics, Exeter, 1962* (The Institute of Physics and The Physical Society, London, 1962), p. 505.

²² D. L. Dexter, in *Solid State Physics*, edited by F. Seitz and D. Turnbull (Academic Press Inc., New York, 1958), Vol. 6, p. 353.

Fe^{2+} ions per unit volume (assumed to equal the total concentration of iron in the crystal), e and m are the electron charge and mass, and c is the speed of light in vacuum. The dashed curves in Figs. 1 and 2 are the estimated curves for the lattice absorption of ZnS as extrapolated from the data above 70 cm^{-1} with the assumption that α for intrinsic ZnS varies as $\bar{\nu}^2$.

IV. THEORY

The ground state of $\text{Fe}^{2+}(3d^6)$ at a substitutional Zn site in cubic ZnS should be the orbital doublet 5E , since the symmetry of the site is tetrahedral (point group T_d). Crystal field theory²³ predicts that 5E should be below 5T_2 for a tetrahedral site, and this order is in agreement with the results of the previous studies.³ Spin-orbit interaction does not split 5E in first order, but in second order (through coupling primarily to 5T_2) it splits 5E into five equally spaced levels with relative energies^{3,4}:

$$\begin{aligned} \text{Level No. 1:} & \quad \Gamma_1(1), \quad E=0, \\ \text{Level No. 2:} & \quad \Gamma_4(3), \quad E=+K, \\ \text{Level No. 3:} & \quad \Gamma_3(2), \quad E=+2K, \\ \text{Level No. 4:} & \quad \Gamma_5(3), \quad E=+3K, \\ \text{Level No. 5:} & \quad \Gamma_2(1), \quad E=+4K. \end{aligned} \quad (4)$$

The splitting interval K is given by crystal field theory to be

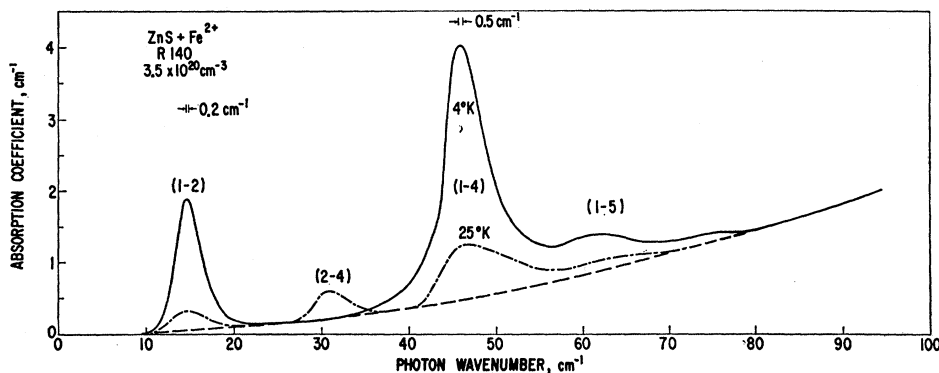
$$K = 6\lambda^2/\Delta, \quad (5)$$

where $\Delta (= 10|Dq|)$ is the cubic field energy separation between 5E and 5T_2 , and λ is the parameter of the effective spin-orbit interaction $\lambda(\mathbf{L} \cdot \mathbf{S})$ between 5E and 5T_2 . The levels in (4) are labeled by the irreducible representations of T_d to which they belong (Beth's notation), and the degeneracy of each level is noted in parentheses. The lowest level for Fe^{2+} in ZnS is the singlet Γ_1 .

Jahn-Teller effects are potentially important in a state such as 5E having orbital degeneracy, but there

²³ D. S. McClure, in *Solid State Physics*, edited by F. Seitz and D. Turnbull (Academic Press Inc., New York, 1959), Vol. 9, p. 399.

FIG. 2. The optical absorption of natural cubic ZnS crystal R140 versus wave number at several temperatures. The transitions principally responsible for the various peaks are indicated by (A-B). The spectrometer resolution is indicated.



was no indication in the previous optical studies³ of Fe^{2+} in ZnS that such effects caused any marked change in the relative energies of the spin-orbit levels of 5E as given in (4). This conclusion is given further support by the measurements reported in this paper. The conditions necessary for a static Jahn-Teller distortion in the 5E state of tetrahedral Fe^{2+} have been discussed by Goodenough.²⁴ He has shown that the anisotropy tending to stabilize a distorted configuration should in fact be weaker for an isolated tetrahedral Fe^{2+} ion than in the corresponding case of an octahedral complex involving for example Cu^{2+} . In agreement with this conclusion, crystals of FeAl_2O_4 ²⁵ and FeCr_2S_4 ,²⁶ which are normal spinels with the Fe^{2+} at the tetrahedral *A* sites, are found to remain cubic down to liquid-helium temperatures, although FeCr_2O_4 is tetragonal below -138°C .²⁷ However, even when a static Jahn-Teller distortion does not occur, a dynamical Jahn-Teller effect may change the energy levels from those predicted by crystal field theory.²⁸ Such an effect may in particular diminish the splitting interval *K* between the levels (4) from the value given by Eq. (5), without affecting the order of the levels or their uniform spacing.³ For Fe^{2+} in ZnS , however, the interval *K* obtained in the previous studies³ and again in the present work agrees quite well with the crystal-field value in Eq. (5) obtained using the free-ion value for λ and the observed cubic field splitting Δ . While such good agreement may be fortuitous and should not be regarded as conclusive proof that Jahn-Teller effects are entirely negligible in the 5E state, in this paper we shall for simplicity ignore Jahn-Teller effects in calculating the oscillator strengths for transitions among the various levels. As we shall see, the agreement between the oscillator strengths calculated on the basis of crystal field theory and the experimental values is reasonably good, but of course the limits of uncertainty for the experimental intensities

are broad enough to preserve this agreement even if the calculated value should be subject to appreciable correction. Dynamical Jahn-Teller effects may in fact help account for some features of the experimental results which do not appear to be wholly in accord with the crystal field theory. An attempt to assess more precisely the importance of such effects in the 5E state will, however, be left to future investigation.

Optical transitions among the levels Nos. 1-5 of 5E occur by both magnetic- and electric-dipole processes. The transitions allowed by the formal selection rules²⁹ for such processes are shown by arrows in Fig. 3. The magnetic-dipole transitions among these levels arise predominantly from the coupling $2\beta\mathbf{S}\cdot\mathbf{H}$ of the spin *S* to the magnetic vector *H* of the incident light. Electric-dipole transitions would not occur at all if the wave functions of the levels (4) were pure 5E , since the electric-dipole moment (like the orbital angular mo-

TABLE II. The absorption peaks of Fe^{2+} in cubic ZnS in the far infrared. (A-B) is the pair of spin-orbit levels giving rise to the transition principally responsible for the absorption peak; *A* = lower level, *B* = upper level; *T* is the temperature at which absorption was measured; $\bar{\nu}$ is the wave number at the absorption peak; α_{max} is the optical absorption coefficient at absorption peak, corrected for background absorption in the ZnS ; *W* is the width of absorption peak at $\alpha = \frac{1}{2}\alpha_{\text{max}}$; *I* is the normalized intensity of the absorption line as defined in Eq. (3).

| Sample | Transition | <i>T</i> (°K) | $\bar{\nu}$ (cm ⁻¹) | α_{max} (cm ⁻¹) | <i>W</i> (cm ⁻¹) | <i>W</i> / $\bar{\nu}$ | 10 ³ <i>I</i> |
|--------|------------|---------------|---------------------------------|---|------------------------------|------------------------|--------------------------|
| R118 | (1-2) | 4.2 | 14.6±0.2 | 0.5 | 1.5 | 0.10 | 6.6 |
| | (2-4) | 25 | 31.1±0.3 | 0.1 | 3.5 | 0.11 | 2.8 |
| | (1-4) | 4.2 | 45.1±0.2 | 1.2 | 5.2 | 0.12 | 55 |
| | | 12 | 45.0±0.2 | 1.1 | 4.7 | 0.10 | 41 |
| | | 25 | 43 ± 1 | 0.5 | 5.0 | 0.11 | 20 |
| | (1-5) | 4.2 | 60 ± 5 | 0.05 | 10 | 0.16 | 5.2 |
| R140 | (1-2) | 4.2 | 14.6±0.2 | 1.8 | 3.5 | 0.24 | 5.8 |
| | | 25 | 14.8±0.4 | 0.3 | 4.5 | 0.30 | 1.0 |
| | (2-4) | 25 | 30.8±0.3 | 0.4 | 4.7 | 0.15 | 1.4 |
| | (1-4) | 4.2 | 45.9±0.2 | 3.5 | 5.6 | 0.12 | 21 |
| | | 25 | 46.4±0.3 | 0.8 | 8.6 | 0.19 | 5.3 |
| | | (1-5) | 4.2 | 60.9±0.5 | 0.4 | 10 | 0.16 |
| 25 | 63 ± 2 | | 0.2 | 5 | 0.08 | 1.1 | |

²⁴ J. B. Goodenough, *J. Phys. Chem. Solids* **25**, 151 (1964).

²⁵ W. L. Roth, *J. Phys. (Paris)* **25**, 507 (1964).

²⁶ G. Shirane, D. E. Cox, and S. J. Pickart, *J. Appl. Phys.* **35**, 954 (1964).

²⁷ E. R. Whipple and A. Wold, *J. Inorg. Nucl. Chem.* **24**, 23 (1962).

²⁸ F. S. Ham, *Phys. Rev.* **138**, A1727 (1965).

²⁹ Reference 3, Table IX.

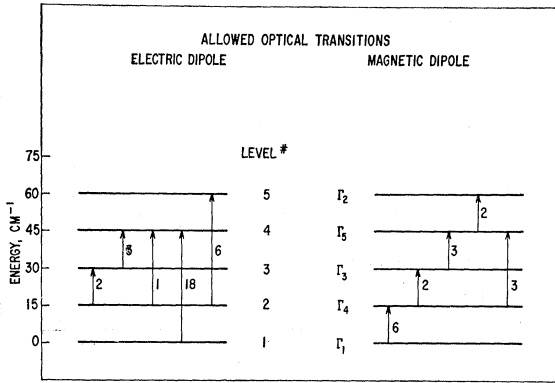


FIG. 3. Allowed transitions (arrows) among the spin-orbit levels of the 5E term of Fe^{2+} ions in ZnS permitted by the selection rules for electric- and magnetic-dipole processes. Transitions between levels not joined by an arrow in the figure are forbidden under the indicated process. The numbers accompanying the arrows are the values for the relative oscillator-strength parameters $f_e(A,B)$ and $f_m(A,B)$ [Eqs. (13) and (16) of the text] appropriate to the transition from the lower to the upper level (initial state A to final state B).

mentum) has no nonzero matrix elements among the orbital doublet states of 5E . However, the spin-orbit interaction responsible for splitting 5E admixes appropriate combinations of the 5T_2 wave functions into the states (4). Since the odd part of the tetrahedral crystal field has broken down the parity selection rule to make ${}^5E \rightarrow {}^5T_2$ transitions electric-dipole allowed and fairly strong,³ this spin-orbit mixing of 5T_2 with 5E provides a very effective mechanism making possible electric-dipole transitions among the levels (4).

The absorption coefficient $\alpha(\bar{\nu})$ resulting from induced transitions among the levels Nos. 1–5 of the Fe^{2+} is given²² by

$$\alpha(\bar{\nu}) = \frac{\pi N e^2 h}{m c n} \left(\frac{\mathcal{E}_{\text{eff}}}{\mathcal{E}} \right)^2 \sum_{A,B} d_A \left(\frac{x_A}{d_A} - \frac{x_B}{d_B} \right) \times f(A,B) S(E_B - E_A - h c \bar{\nu}). \quad (6)$$

Here x_A is given by

$$x_A = \frac{d_A \exp(-E_A/kT)}{\sum_B d_B \exp(-E_B/kT)}$$

and is the fraction of the Fe^{2+} ions which at thermal equilibrium is in the level A , which has energy E_A and degeneracy d_A . $S(t)$ is a line-shape function which is nonzero only for $t \approx 0$ and normalized such that $\int_{-\infty}^{\infty} S(t) dt = 1$. The oscillator strength of the transition from level A to level B is denoted by $f(A,B)$, and the summations in Eq. (6) should be taken over the five levels given in (4). Since $\bar{\nu}$ is taken to be positive, the function $S(E_B - E_A - h c \bar{\nu})$ restricts the terms contributing to Eq. (6) to those for which $E_B > E_A$. Because both levels

involved in a given transition may be populated in thermal equilibrium, the expression (6) has been written to take account of stimulated emission as well as of absorption.

The oscillator strength $f(A,B)$ may be separated into two parts

$$f(A,B) = f_e(A,B) + f_m(A,B), \quad (7)$$

arising, respectively, from electric- and magnetic-dipole transitions. For the former we have

$$f_e(A,B) = (4\pi m c \bar{\nu}_{BA} / h d_A) \sum_{a,b} |\langle A a | \mathbf{R} \cdot \hat{\epsilon} | B b \rangle|^2, \quad (8)$$

where $h c \bar{\nu}_{BA} = (E_B - E_A)$, $\hat{\epsilon}$ is a unit vector in the direction of polarization of the light, and $\mathbf{R} = \sum_j \mathbf{r}_j$ is the sum of the coordinate operators of the electrons of the Fe^{2+} ion. The summation in Eq. (8) extends over the degenerate states a and b comprising levels A and B , respectively. The contribution of the magnetic-dipole processes to Eq. (7) is

$$f_m(A,B) = \frac{h \bar{\nu}_{BA} n^2}{2 m c d_A} \left(\frac{\mathcal{E}}{\mathcal{E}_{\text{eff}}} \right)^2 \times \sum_{a,b} |\langle A a | (\mathbf{L} + 2\mathbf{S}) \cdot (\hat{\epsilon} \times \hat{k}) | B b \rangle|^2, \quad (9)$$

where \hat{k} is a unit vector in the direction of propagation of the light, and $\hbar \mathbf{L}$ and $\hbar \mathbf{S}$ are the electronic orbital and spin angular-momentum operators, respectively, of the Fe^{2+} ion. The factor $(\mathcal{E}/\mathcal{E}_{\text{eff}})^2$ appears in Eq. (9) in order to compensate the factor $(\mathcal{E}_{\text{eff}}/\mathcal{E})^2$ appearing in Eq. (6); no local-field correction is required for a magnetic-dipole transition because the coupling is with the magnetic vector of the light. The appearance of this factor in the expression (9) for the magnetic-dipole contribution to the oscillator strength is awkward, but it is necessary so long as we follow the usual practice of defining the oscillator strength of the optical transition in terms of the strength of the equivalent classical electric-dipole oscillator.

The matrix elements of \mathbf{R} , which according to Eq. (8) give the electric-dipole part of the oscillator strength for transitions among the five levels (4), are different from zero because the spin-orbit interaction $\lambda(\mathbf{L} \cdot \mathbf{S})$ admixes the wave functions of 5T_2 into those of 5E in proportion to λ/Δ . It has been shown elsewhere³ that the matrix elements of \mathbf{R} between 5E and 5T_2 depend upon a single parameter, and that this parameter can be obtained from the measured oscillator strength of the ${}^5E \rightarrow {}^5T_2$ optical absorption band. It is accordingly possible to relate the electric-dipole intensities of the transition among the levels (4) to the observed oscillator strength of the ${}^5E \rightarrow {}^5T_2$ band (unless, of course, other excited states besides 5T_2 are mixed appreciably with 5E by the spin-orbit interaction—we shall assume these

can be neglected since they lie at substantially higher energy than 5T_2 and should have very small values for the matrix elements with 5E of either the electric-dipole moment or the spin-orbit interaction or both). We introduce the parameter a^2 defined³⁰ by

$$a^2 = (4\pi^2 m \Delta / \hbar^2) |\langle E\theta | R_z | T_{2\zeta} \rangle|^2 \quad (10)$$

(where $\langle E\theta | R_z | T_{2\zeta} \rangle$ is a particular matrix element of \mathbf{R} between the orbital wave functions of the 5E and 5T_2 states). It has been shown³ that a^2 is given to a good approximation by the total oscillator strength of the ${}^5E \rightarrow {}^5T_2$ absorption band,

$$a^2 = F_{\text{tot}}({}^5E \rightarrow {}^5T_2). \quad (11)$$

The previous measurements³ found that for Fe^{2+} in ZnS

$$a^2 = 6.4 \times 10^{-4}. \quad (12)$$

It is then straightforward to obtain the spin-orbit admixtures of the 5T_2 wave functions to the states (4) of 5E and to calculate the electric-dipole oscillator strengths (8) among these levels in terms of a^2 . We may express these oscillator strengths as

$$f_e(A, B) = p_e(A, B) C_e, \quad (13)$$

where the numbers $p_e(A, B)$ are given in Fig. 3, and C_e is defined by

$$C_e = (4/9)(K/\Delta)^2 a^2. \quad (14)$$

In putting the results in the form (13), we have related the ratio λ^2/Δ to K by means of Eq. (5), and we have used the energy separations of the levels as given in (4). From the values for K , Δ , and a^2 found in the previous work,³ we obtain the value

$$C_e = 5.7 \times 10^{-9}. \quad (15)$$

The magnetic-dipole part of the oscillator strengths may be related to a single parameter and expressed in a form similar to Eq. (13),

$$f_m(A, B) = p_m(A, B) C_m, \quad (16)$$

if we ignore the contribution of the orbital angular momentum \mathbf{L} to the matrix elements in Eq. (9) in comparison to that of the spin. This is a good approximation, since the matrix elements of \mathbf{L} among the levels (4) are diminished in proportion to the ratio (λ/Δ) . We define C_m then as

$$C_m = (2Kn^2/3mc^2)(\mathcal{E}/\mathcal{E}_{\text{eff}})^2 \quad (17)$$

and give the numbers $p_m(A, B)$ in Fig. 3. Substituting values for the parameters in Eq. (17), we obtain for C_m the value

$$C_m = 1.7 \times 10^{-9}. \quad (18)$$

³⁰ Reference 3, Eq. (4.15) and footnote 75.

V. INTERPRETATION OF RESULTS

At the lowest temperatures almost all the Fe^{2+} ions should be in the ground-state singlet Γ_1 (level No. 1), the lowest of the five levels given in (4). From Fig. 3 we see that there are only two allowed transitions from this level, an electric-dipole transition (1-4) to the Γ_5 triplet at $E=3K$, and a magnetic-dipole transition (1-2) to the Γ_4 triplet at $E=K$. At 4.2°K, therefore, we would expect to see only two peaks in the absorption spectrum in the far infrared, the first at one-third the wave number of the second. This expectation is in good agreement with the observation of the two prominent peaks in Figs. 1 and 2 near 15 and 45 cm^{-1} . As the crystal is warmed, the number of Fe^{2+} ions in level No. 2 should become appreciable, and we expect from Fig. 3 that a new absorption line (2-4) should appear at a wave number two-thirds that of the higher original peak, corresponding to both electric- and magnetic-dipole transitions from the lower triplet Γ_4 to the higher triplet Γ_5 . Such a line is in fact apparent in Figs. 1 and 2 at 25°K, near 31 cm^{-1} .

From the observed positions (Table II) of these three peaks we obtain the value

$$K = 15.2 \pm 0.4 \text{ cm}^{-1} \quad (19)$$

for the energy interval between the levels (4). This agrees with the value $K = 15 \pm 2 \text{ cm}^{-1}$ obtained from the previous optical studies³ in the near infrared. Making use of Eqs. (5) and (19) and the previously obtained value³ for $\Delta = 3400 \text{ cm}^{-1}$, we obtain a value for the effective spin-orbit parameter

$$|\lambda| = 93 \pm 1 \text{ cm}^{-1}, \quad (20)$$

which is close to the free-ion value³¹ $\lambda = -100 \pm 10 \text{ cm}^{-1}$.

From the normalized intensities (Table II) of the observed absorption peaks (1-2) and (1-4) at 4.2°K, we may obtain from Eqs. (13) and (16), and from the values for $p_e(1,4)$ and $p_m(1,2)$ in Fig. 3, experimental values for the parameters C_e and C_m , which determine the absolute value of electric- and magnetic-dipole transitions, respectively, among the five levels (4). These values are given in Table III, where they are

TABLE III. Comparison of experimental and theoretical values for the electric- and magnetic-dipole oscillator-strength parameters C_e and C_m for optical transitions within 5E .

| Source | $10^\circ C_e$ | $10^\circ C_m$ |
|-------------|----------------|----------------|
| Experiment | | |
| Sample R118 | 3.1 | 1.1 |
| Sample R140 | 1.2 | 1.0 |
| Theory | 5.7 | 1.7 |

³¹ C. E. Moore, *Atomic Energy Levels*, Natl. Bur. Std. (U.S.) Circ. No. 467 (U. S. Government Printing and Publishing Office, Washington, D. C., 1952), Vol. 2, p. 60.

compared with the theoretical values (15) and (18). The agreement between theory and experiment is within a factor of 2 for C_m for both samples and for C_e for the sample R118 with the lower iron concentration, the experimental value in all cases being smaller than the theoretical one. For sample R140 the agreement for C_e is only to within a factor of 5.

Although the transition (1-5) is forbidden for both electric- and magnetic-dipole processes, there is evidently some absorption due to the iron in both Figs. 1 and 2 in the vicinity of 60 cm^{-1} . We are unable to account for this absorption on the basis of the model for isolated Fe^{2+} , but we believe it may arise from Fe^{2+} pairs since this absorption is more prominent in the sample with the higher iron concentration, or else from Fe^{2+} associated with some crystal imperfection. A value for the intensity I of this line is included in Table II for completeness, where it is labeled (1-5) because of its position. In sample R118, this line is somewhat difficult to distinguish from the background ZnS absorption and the wing of the peak (1-4).

As the crystal is warmed above liquid-helium temperatures, the higher levels (Nos. 2-5) of the Fe^{2+} ion become populated. Since the energy separation of the levels (4) is uniform, we see from Fig. 3 that transitions between several different pairs of levels now contribute

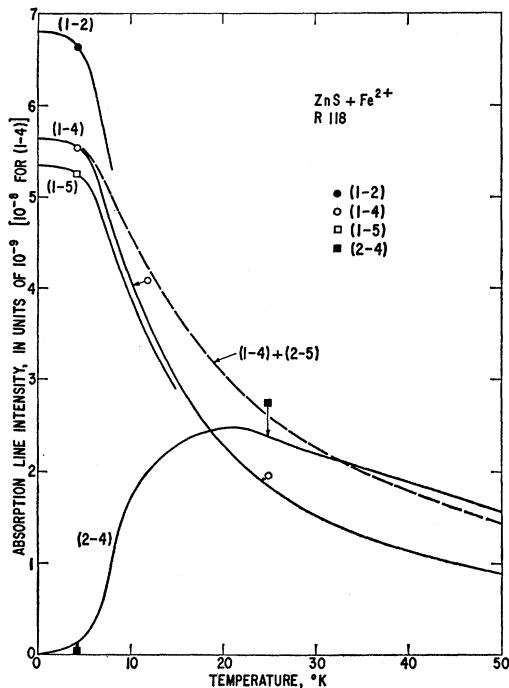


FIG. 4. The integrated band intensities I versus temperature T for crystal R118. The points are experimental. The solid lines are the theoretical curves for I versus T as matched to the 4.2°K results for the (1-2), (1-4), and (1-5) transitions. These solid curves have been calculated for the single transition as shown. The dashed curve shows the theoretical results for the 45-cm^{-1} band if the calculated intensities for both the (1-4) and (2-5) transitions are added.

to a single absorption peak. Moreover, since the higher level of each pair may now be appreciably populated, we must calculate the net absorption taking account of stimulated emission. Comparing our expression (3) for the normalized intensity I of an absorption peak with Eq. (6) for the absorption coefficient, we find that I is given in terms of the oscillator strengths of the various transitions by

$$I = \sum'_{(A,B)} d_A \left(\frac{x_A}{d_A} - \frac{x_B}{d_B} \right) f(A,B), \quad (21)$$

where the primed summation is over those pairs of

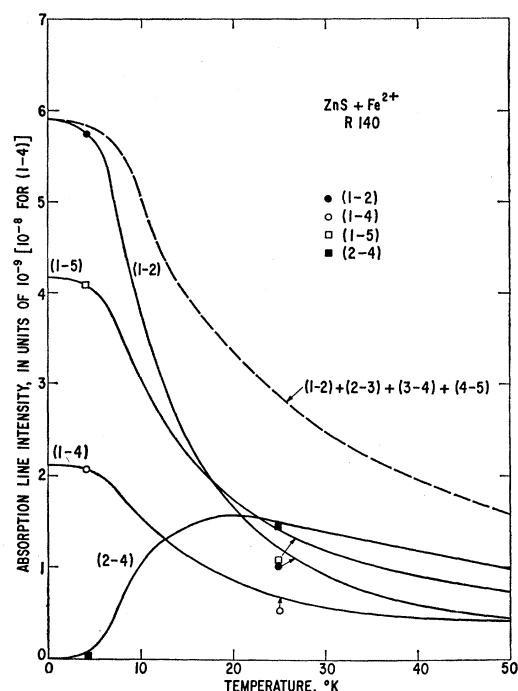


FIG. 5. The integrated band intensities I versus temperature T for crystal R140. The points are experimental. The solid lines are the theoretical curves for I versus T as matched to the 4.2°K results for the (1-2), (1-4), and (1-5) transitions. These solid curves have been calculated for the single transition as shown. The dashed curve shows the theoretical results for the 15-cm^{-1} band if the calculated intensities for the four transitions (1-2), (2-3), (3-4), and (4-5) are all added.

levels which have the proper separation to contribute to a given peak. We have used Eq. (21) to calculate the expected intensity of the various peaks as a function of temperature, using the appropriate Boltzmann factors x , as given following Eq. (6), and the oscillator strengths as given by Eqs. (7), (13), and (16). The values for C_e and C_m used in this evaluation were the experimental values obtained for the given sample at 4.2°K and tabulated in Table III. The results of this calculation are shown in Figs. 4 and 5. The solid lines show the contribution to I from the single pair of levels (including

stimulated emission) which dominates a given absorption peak at the lower temperatures (and according to which the peak is labeled in Figs. 1 and 2), while the dashed lines show the total value expected for I when Eq. (21) is summed over all participating pairs. The points show the experimental values. We see that the observed intensity of the peak (2-4) at 25°K agrees very well with that predicted. Peaks (1-2) and (1-4), however, have a lower intensity at 25°K than is predicted when Eq. (21) is summed over the participating pairs of levels. Both of these peaks agree remarkably well at 25°K with the intensity calculated for the single pair (1-2) or (1-4) alone, but this result is probably fortuitous. We might be able to account for such a result if the absorption peaks due to the transitions (2-3), (3-4), (4-5), and (2-5) were several times broader at 25°K than the peaks (1-2) and (1-4), so that only the latter stand out distinctly from what we have taken to be the background ZnS absorption. However, calculation of the effects of random strains in broadening the peaks shows that (1-2), (1-4), (2-3), (2-5), (3-4), and (4-5) should be broadened by strain by the same amount. Moreover, the lifetime of levels Nos. 3, 4, and 5 for nonradiative transitions to lower levels is the same and is shorter than that of level No. 2, so that lifetime broadening would also not suffice to make (2-3), (3-4), (4-5), and (2-5) too broad to be observed so long as (1-4) is as clearly resolved as it is seen to be at 25°K in Figs. 1 and 2.

From the experimental values obtained for the oscillator strengths $f(A,B)$ of the transitions $A \rightarrow B$, we may calculate the lifetimes $\tau_R(B,A)$ of the levels for spontaneous radiative decay via the inverse process $B \rightarrow A$, using the relation³²

$$\frac{1}{\tau_R(B,A)} = \frac{8\pi^2 n \bar{\nu}_{BA}^2 e^2 d_A^2 \left(\frac{\mathcal{G}_{\text{eff}}}{\mathcal{G}}\right)^2}{m c d_B} f(A,B). \quad (22)$$

Table IV lists the values of $\tau_R(B,A)$ derived from the data of Table II for the observed absorption peaks. The radiative lifetimes of levels Nos. 2-5 are accordingly of the order of $\frac{1}{2}$ to 30 h. Since these times are very long compared to lifetimes that we estimate for spontaneous emission of an acoustic phonon, the decay of the excited levels of 5E should be due to nonradiative processes rather than to photon emission.

The agreement between the results of the present measurements and the predictions of crystal field theory is on the whole remarkably good, despite the discrepancies which we have noted. This work, therefore, provides further support for the conclusion from the previous optical studies³ that crystal field theory gives

TABLE IV. Lifetimes for spontaneous radiative decay of excited levels of 5E , derived from experimental values of the oscillator strength of the observed absorption peaks.

| Absorption peak (A-B) | Transition type ^a | Oscillator strength ^b $f(A,B) \times 10^6$ | Radiative lifetime ^c $\tau_R(B,A)$ (hours) |
|-----------------------|------------------------------|---|---|
| (1-2) | <i>m</i> | 6 | 28 |
| (1-4) | <i>e</i> | 40 | 0.5 |
| (1-5) | ? | 5 | ~0.7 |
| (2-4) | <i>e+m</i> | 6 | 2 |

^a *e* = electric dipole; *m* = magnetic dipole.

^b The value given for $f(A,B)$ is that obtained using Eq. (21) of the text from the value for I given in Table II, averaged for the two samples: the 4.2°K data was used for transitions (1-2), (1-4), and (1-5), and the 25°K data for (2-4).

^c The radiative lifetime was calculated from the value for $f(A,B)$ using Eq. (22) of the text.

a quite good description of the 5E ground state for Fe^{2+} in ZnS. The agreement between the value (20) for the effective spin-orbit parameter λ obtained from the level separation K and the free-ion value is especially noteworthy. If dynamical Jahn-Teller effects are present in 5E to any significant extent, they evidently act to reduce K by less than some 20 to 30%, unless of course for some reason K in the absence of Jahn-Teller coupling should be larger than given by Eq. (5), or the effective $|\lambda|$ larger than the free-ion value. On the other hand, a dynamical Jahn-Teller effect would tend to further improve the agreement between the theoretical and experimental values for C_e and C_m given in Table III, since such an effect would act to transfer some of the oscillator strength of (zero-phonon) transitions among levels Nos. 1-5 to transitions involving the simultaneous emission or absorption of a lattice phonon. Thus an appreciable dynamical Jahn-Teller effect would reduce the experimental values of C_e and C_m obtained from the zero-phonon line intensities, in agreement with the consistent sense of the discrepancy in Table III. However, this discrepancy may of course simply be because some of the iron in the crystals is not in the form of isolated Fe^{2+} ions and therefore does not contribute to the observed absorption. Finally, the discrepancies noted in Figs. 4 and 5 with respect to the line intensities at 25°K might perhaps be due to some intensity loss to the background resulting from transitions in which a phonon is absorbed, such transitions again being made allowed by the Jahn-Teller coupling. These discrepancies may, on the other hand, occur because states other than 5T_2 are admixed appreciably with 5E by the spin-orbit interaction and thereby change the relative oscillator strengths of the electric-dipole transitions from those given by Eq. (13).

ACKNOWLEDGMENT

The authors wish to thank J. H. McTaggart for his help in preparing the optical samples.

³² W. B. Fowler and D. L. Dexter, Phys. Rev. **128**, 2154 (1962).